# Power Transformer Diagnosis based on Mechanical Oscillations due to AC and DC Currents

**Michael Beltle, Stefan Tenbohlen**
University of Stuttgart
Institute of Power Transmission and High Voltage Technology (IEH)
Pfaffenwaldring 47
70569 Stuttgart, Germany

## ABSTRACT

**The reliable operation of power transformers is an essential factor for the high availability of electric energy. Reliability demands can be enforced using condition based asset management which relies on different diagnosis measurements and continuous monitoring. This contribution determines the abilities of asset monitoring by regarding transformers' mechanical oscillations during operation. The physical origins of oscillation sources are introduced as well as the common measurement technique using accelerometers. The contribution evaluates the method's principle diagnostic abilities by correlating the actual mechanical status of an active part and resulting mechanical vibrations in a laboratory setup. The practical usability is determined by long-term comparison of measurements on different power transformers in service. Several influencing factors are evaluated: the sensor position, the changing transformer's load and operating temperature during service as well as the position of the on-load tap changer. Additionally, mechanical oscillations are used to determine the influence of superimposed, undesirable DC components on 3-limb power transformers originated by coupling between nearby AC and HVDC lines.**

Index Terms - **Power transformers, monitoring, vibration measurement, magnetostriction, magnetic hysteresis, magnetic noise, HVDC transmission lines.**

## 1 INTRODUCTION

**MECHANICAL** oscillations of transformers during operation are mostly recognized for being the cause of transformer noises [1]. They are taken into consideration during design process to avoid core geometries which would enforce mechanical resonances at excitation frequencies and hence could lead to critical mechanical forces to the structure [2]. Concerning asset management, the question arises if they can be applied as a tool to determine transformers' mechanical status during service. Condition based asset management is gaining importance, which leads to a prospering of power transformer monitoring [3, 4]. Different methods, for example the dissolved-gas-analysis [5], partial discharge measurements [6] and also frequency response analysis [7] have been established to determine the status of the electric insulation and windings. In theory, vibration analysis during operation allow to survey mechanics, since they are either originated by the structure (windings and core) or lie within the signal path (e.g. the mounting of the active part in the tank). Different publications show the correlation between mechanical status and oscillations, for example in a small test setup using a resin impregnated transformer [8]. Also, changing mechanical oscillations driven by winding defects have been evaluated [9, 10]. In most evaluations accelerometers on the tank surface are used, but some research also consider local measurements directly on winding or core using optical strain sensors [11, 12]. Besides monitoring during service, some approaches determine transient oscillations when transformers are empowered to derive information about the mechanical status [13]. This contribution provides a detailed evaluation of influencing factors which have to be considered on both, mechanical oscillation measurement on the tank surface and monitoring during service to enable asset surveillance.

## 2 PHYSICS OF MECHANIC OSCILLATIONS

The mechanical oscillation of the tank walls origins in the periodical movement of both, windings and core sheets under the influence of the magnetic field which couples through the structure and the oil as structure- and fluid-borne sound. The winding movement is driven by the Lorentz Force which depends on the load current. The core movement is driven by magnetostriction. The material of the core's electric steel sheets can be separated into single Weiss' domains in the crystal structure. Each domain has its own magnetic polarisation $I_{mag}$.

*Manuscript received on 29 July 2015, in final form 25 January 2016, accepted 1 February.*

*DOI: 10.1109/TDEI.2016.005537*

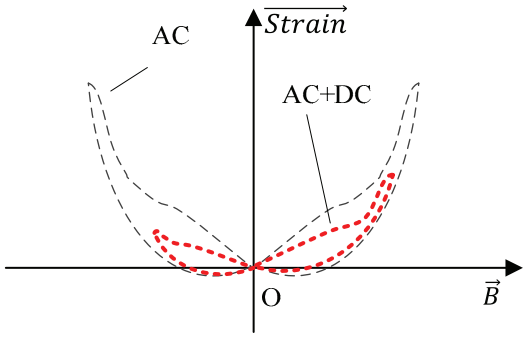


**Figure 1.** Butterfly curve: general alternation of length in one direction against applied magnetic flux density inside a ferromagnetic material at AC only (black) and superimposed AC+DC condition (dotted, red).

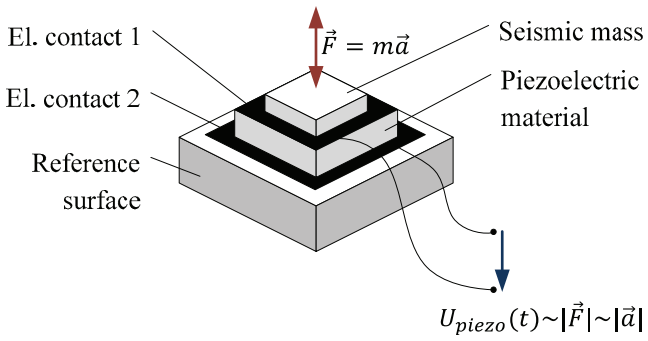


**Figure 2.** Working principle and different layers of a 1-dimensional piezoelectric sensor used to measure acceleration orthogonal to the reference surface.

In a non-magnetized ferromagnetic material all polarisations superimpose destructively and the macroscopic behaviour is neutral. The domains align themselves along an external applied magnetic field $H$. Every domain claims a specific volume and size in the material. Depending on the steel type and treatment during production, domain sizes can differ. If the externally applied magnetic field $H$ changes, the domains follow the field by either movement of their boundaries (the Bloch-Walls) or by a rotation of the domains [14]. The summarized volume of all domains remains constant, thus wall movement and rotation lead to a mechanical deformation. If the applied external field alternates sinusoidal, so do the domains align themselves. Hence, in each period of the magnetic flux each Weiss' domain has a certain orientation twice, which leads to a mechanical oscillation with doubled electric frequency [15]. An electrical frequency of $f_{n,\,voltage} = 50$ Hz leads to an equal magnetic frequency $f_{n,magnetic\,flux} = 50$ Hz but to a doubled mechanical oscillation $f_{n,core} = 100$ Hz. The working principle for AC only excitation is shown in the Strain-$B$ diagram shown in Figure 1.

### 2.1 MEASUREMENT TECHNIQUE

A common way to measure mechanical oscillations is performed by a piezoelectric accelerometer of which Figure 2 shows the schematic sketch. The sensor is fixed on the reference surface. Its lower part moves with the surface, if the mechanical force $F$ is applied. The seismic mass element is an inertial mass and does not follow the movement. Hence, the piezoelectric material in between is compressed which leads to an electric potential difference between the contacts. The shown sensor is 1-dimensional and is only sensitive to forces perpendicular to the reference surface. The resulting generated electric potential between the contacts depends on the used material properties and the compressed volume which leads to a constant proportional factor $k$.

The measured voltage can be derived from the generated charge and the overall capacity of the sensor which includes the plate capacity between the electrodes $C_0$ and all occurring stray capacities $C_s$.

$$u = \frac{q}{C} = \frac{kF}{C_0 + C_S} \qquad (1)$$

The typical sensor frequency range is similar to the audible spectrum up to approx. 20 kHz with an average sensitivity of $k_{sens} \approx 10$ mV / (m/s²). As Figure 15 (reference spectrum) shows, mechanical oscillations of significant amplitude reach up to several 100 Hz. Frequencies < 1 kHz cover about 95 % of the entire signal power. Hence, the sensors are considered as suited for the application. Usually, the sensor signals require low noise amplification, especially for low level accelerations in a laboratory setup. Afterwards, signals can be digitized and converted into frequency domain using Fast Fourier Transformation (FFT).

## 3 SENSITIVITY OF SURFACE TANK MEASUREMENTS

The correlation of the mechanical status of the active part's core and measured vibrations is determined in a laboratory setup which allows the manipulation of clamping torque of the core. The influence on the mechanical oscillations is evaluated at the basic mechanical frequency $f_{n,mech} = 100$ Hz. Core magnetisation is provided by an 3-phase voltage source.

### 3.1 LABORATORY EVALUATION

The transformer under test is a modified 7.5 kV / 400 V Yy0 distribution transformer with a full overlap stacked core suspended from the cover. Two acceleration sensors are attached on the core yoke, see Figure 3 A) and B). Sensor $S_V$ is attached on the middle of the yoke, above the limb of phase V. Sensor $S_W$ is positioned above outer phase W. The third sensor $S_{ext}$ is attached on the outside tank wall, see Figure 3 C) which is a typical position for onsite, online measurements [16]. The transformer is energised on its HV side using an adjustable three phase 0-7 kV AC source at nominal frequency $f_n = 50$ Hz. The transformer's 400 V side is in open circuit. The sheets of the core are fixed with several threaded bolts on the active part's general structure, see Figure 4. The torque of each bolt can be alternated. For each test of the applied series, the active part is pulled out of the tank, torques are adjusted and the active part is reinstalled into the tank.

Because the intention is to monitor transformers online during service, the experiments are performed at steady state, idle condition of the test transformer. Other experiments have already determined mechanic oscillations at transient operation (at switch-on) [13].

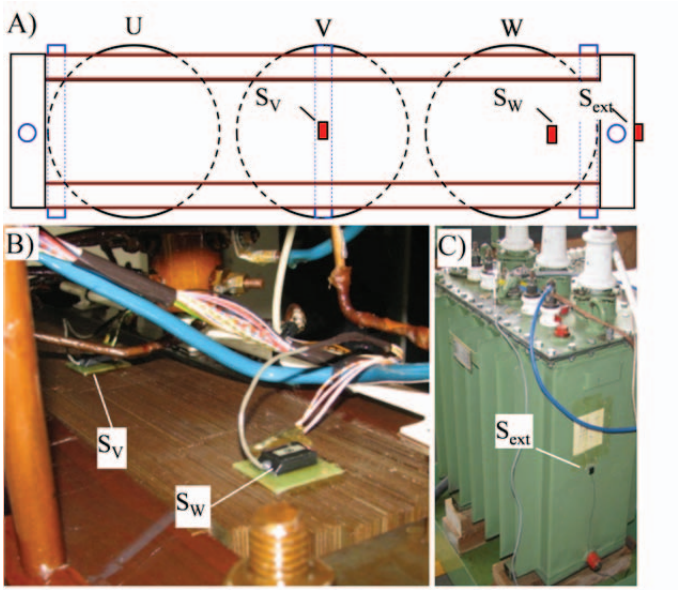


**Figure 3.** Laboratory measurement setup with 2 accelerometers on the core yoke and one external sensor on the side tank wall. A) Top view schematic B) Sensors attached on the upper yoke C) Side view with external sensor.

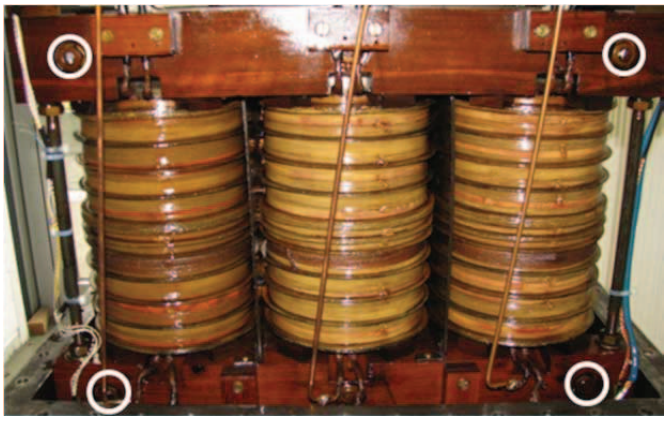

**Figure 4.** Active part of test transformer. Threaded bolts (see marking) apply horizontal clamping forces to the core sheets.

Three different setups of torque are determined: the original torque (14 Nm), a reduced torque (0 Nm) and a tightened torque (45 Nm). The resulting basic mechanical frequency $f_{n,mech} = 100$ Hz at the different torques is shown in Figure 5. The comparison of the original core torque and the loosened setup shows highest oscillations at the outer limb at phase W. Also, local oscillations at phase W show a non-linear dependency to the supply voltage, which results in decreasing signal power at rising source voltage for excitation levels above 5 kV. Mechanical oscillations are lowest at high torque, because a threaded bolt tightens the core in close proximity to the position of sensor $S_W$. The measurements obtained from the geometric centre of the setup (sensor $S_V$) show only small changes between the original and loosened setup because the distance between threaded bolts and sensor is high compared to the others. Changes can only be detected at high torque, where the signal power decreases. The signals measured on the outside tank wall using $S_{ext}$ show a different behaviour.

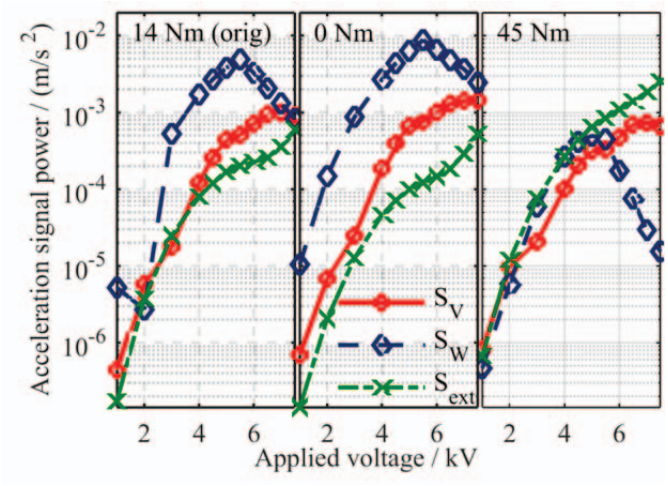


**Figure 5.** Signal power of 100 Hz acceleration at different positions during tests with original (left), loosened (middle) and tightened clamping forces (right) vs. rising AC excitation voltages.

Signal power increases for high torque due to the rising mechanical coupling which provides a signal path with low attenuation through the solid structure. All determined changes of the torque lead to a different structure borne mechanical oscillation measured directly on the active part or the tank. Signals at different positions are not influenced uniformly, but individually, depending on the sensor position. Hence, it is not possible do derive local mechanical oscillations from the tank measurement but structural changes can be identified by deviations at each position generally.

### 3.2 ONSITE, ONLINE MEASUREMENTS

The sensors used for onsite, online measurements are the same as in the previous laboratory test setup. The normal component of mechanical displacement of the tank wall can is recorded in time domain. Figure 6 shows a typical onsite, online measurement setup using two sensors. Basically, it is the same as for laboratory measurements, except the lack of the Supervisory Control and Data Acquisition (SCADA) system and the internal Fourier Transformation. Signal amplification uses low noise amplifiers (LNAs). Recording and Fast Fourier Transformation are performed online, whereas the correlation to operation data is part of the post processing.

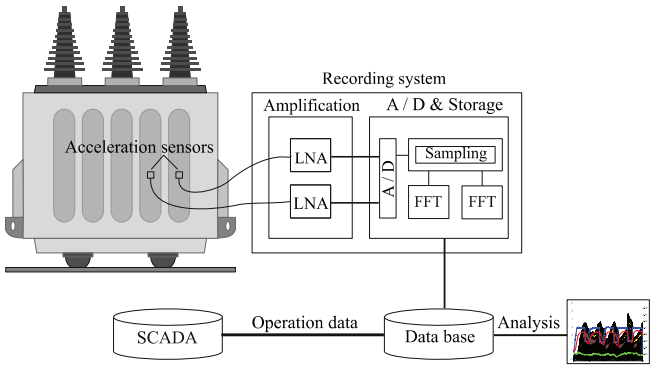


**Figure 6**. Acceleration measurement setup for online long-term tank wall measurements.

### 3.3 INFLUENCE OF SENSOR POSITIONS

The correlation between multiple measurement points on a tank wall and the resulting acceleration signal is performed on a power transformer in service. Figure 7 shows the side view of a 5-limb power transformer which provides 10 wall segments.

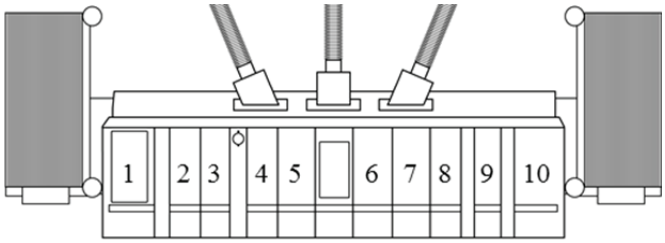


**Figure 7**. External sensor locations 1-10 on a 400 kV / 110 kV power transformer.

Acceleration is measured at each segment at the same height and always in the middle of a segment. The boundary conditions for all measurements are the same: constant temperature, constant load factor of the transformer and same tap changer position. Oil pumps are running but not the fans of the air cooling system. The signal power is discriminated into the basic frequency (100 Hz), harmonic contents, sub harmonics and noise. Figure 8 shows the frequency dependent quadratic power density, which can be summarized to obtain the entire quadratic density. Harmonics are shown up to the 4th (400 Hz) harmonic. Due to the small signal power at higher orders, the 5th to 25th harmonics are plotted summarized. For the same reason noise is neglected. Odd subharmonics are also plotted summarised (50 Hz, 150 Hz, …, 550 Hz).

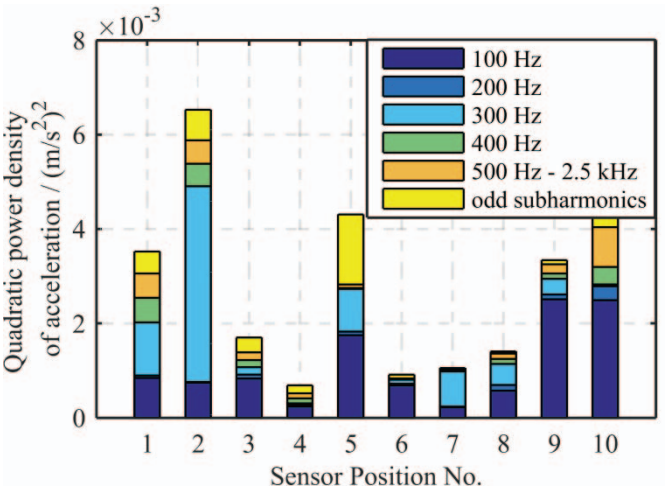


**Figure 8.** Power density distribution of acceleration signals at different sensor locations, compare positions to Figure 7.

Both, the entire quadratic signal power and single frequency components at each position show high variations. There is a tendency to rising signal power at the edges of the transformer and in the middle (compare segments 1, 2 and 9, 10). The basic frequency can be measured at all positions but does not always provide highest signal levels. Main frequencies providing signal power are the basic frequency and the 3rd harmonic. Because of the usually high signal power of the basic frequency, it will be used in the next chapter. Generally, different punctual tank wall measurements from power transformers cannot be compared directly to each other. Additional distributed vibration measurements on a small test tank are given in [17]; simulations on a mid-range transformer are considered in [18]. Taking the practical use of mechanical monitoring into account, only measurements of one specific location are comparable over time.

### 3.4 INFLUENCE OF TAP CHANGER POSITION

This chapter determines the influence of the on-load tap changer (OLTC) position on the vibration behaviour. Long-term measurements are made at the transformer introduced in chapter 0. The sensor is attached on segment 9 permanently, see Figure 7. Acceleration is recorded every 15 minutes during a 4-month test and is correlated with the tap changer position in post processing. The considered grid coupler only operates in partial load $P < 0.45\,P_N$: Figure 9 shows the basic frequency plotted over the occurred OLTC positions including the mean values and standard deviations at each position. The high standard deviation at each position does not indicate a direct dependency. It is caused by additional effects of load and (oil) temperature, which are discussed in the following chapter 0. The non-linearity between the mean values also indicates no correlation. Similar observations apply for the harmonics (not shown).

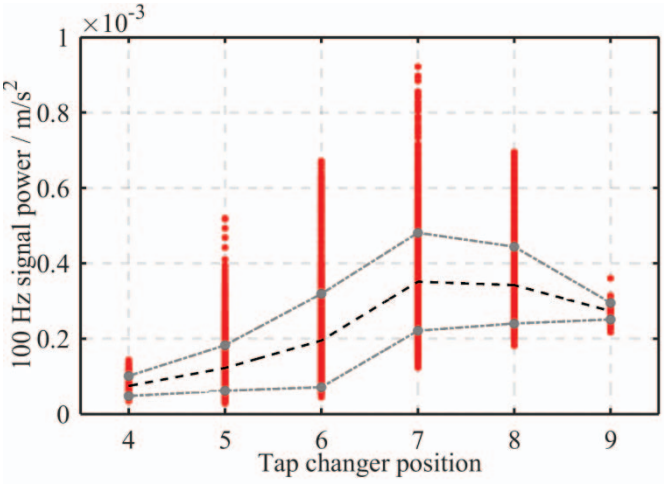


**Figure 9.** Signal power of 100 Hz acceleration of sensor position 9 at different tap changer positions (red dots represent single measurements). Black: mean values; grey: standard deviations for each tap changer position.

Taking the tap changer's regulating mechanism into account the missing correlation is plausible: to keep its 110 kV voltage level constant, the tap changer control tries to compensate voltage changes in the 400 kV level in order to keep the output voltage constant at 110 kV by adding and removing windings for reactive power compensation. Assuming the regulator is successful the magnetic flux has to be constant due to Faraday's law of induction.

### 3.5 INFLUENCE OF LOAD AND TEMPERATURE

Mechanical oscillations correlate with load. The direct link to load is due to the load current driven Lorentz force on the windings. Lorentz force rises quadratically with the current.

Figure 10 shows the quadratic power density of single frequencies against the transformer's apparent power for the same 4-month test introduced in chapter 0. The general dependency only applies for the basic frequency.

Other harmonic contents either diminish with rising load (500 Hz, higher- and subharmonics) or are load-invariant (200 Hz). Therefore, only the basic frequency is determined in detail. Additionally, mechanical oscillations correlate with the oil temperature (which itself depends on the load, cooling and ambient temperature). Temperature influences mechanical oscillations by the expansion and contraction of core sheets and structure materials.

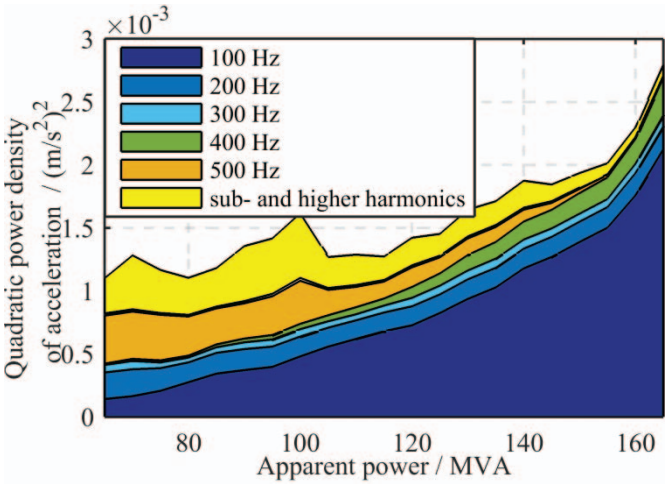


**Figure 10.** Power density distribution of acceleration signals vs. apparent power at sensor location no. 9, see Figure 7.

The different effects of both, load and temperature are derived from two long-term measurements performed on two step-up transformers at different coal power plants. Figure 11 shows the 100 Hz signal power of both transformers. Both measurements are normalized for better comparison. The reference is given by the maximum measured acceleration of each data set. The oil directed, water forced (ODWF) 525 MVA transformer shows a quadratic dependency on the load current, whereas the oil forced, air forced (OFAF) 120 MVA transformer doesn't show any correlation. A direct comparison between both transformers is not possible. Figure 12 shows the same acceleration measurements plotted against the top oil temperature of each transformer.

In this comparison, the smaller OFAF 120 MVA transformer provides a linear dependency between mechanical oscillation and the top-oil temperature from approximately 10°C to 55°C with high variations. The ODWF 525 MVA transformer does not show linear correlation but a cluster from 35°C and 40°C due to the regulated cooling system. Hence, the previously made assumption is becoming more evident: mechanical oscillations cannot be compared between single assets due to the superimposition of factors influencing measurements taken at different transformers. Nevertheless, the laboratory setup in chapter 0 and long-term evaluations on a single transformer presented in [16] illustrate the suitability of mechanical oscillations to detect structural changes in general.

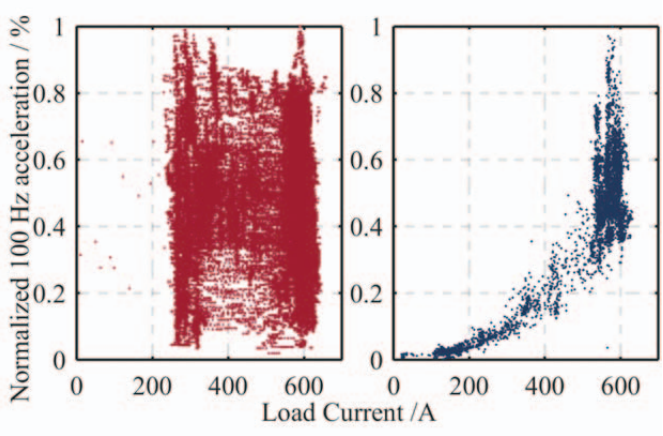


**Figure 11.** Mechanical oscillations vs. transformers' load:
left: 120 MVA OFAF step-up unit; right: 525 MVA ODWF step-up unit

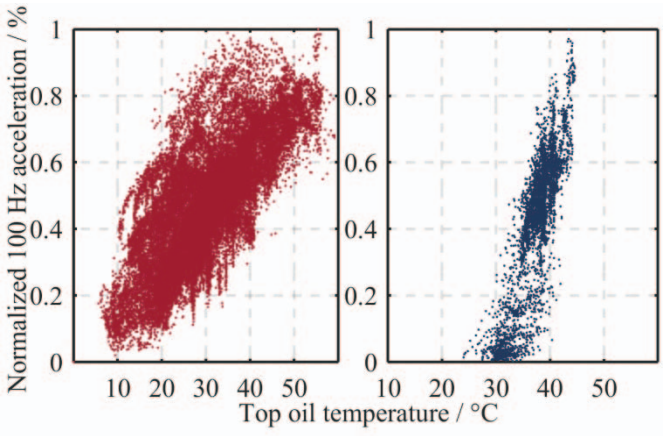


**Figure 12.** Mechanical oscillations vs. transformers' temperature:
left: 120 MVA OFAF step-up unit; right: 525 MVA ODWF step-up unit

## 4 INFLUENCE OF PARASITIC DIRECT CURRENTS

Direct currents are usually not associated with the conventional AC transmission grid. However, some effects cause DC-like currents within the AC grid: Geomagnetically Induced Currents (GIC) [19], [20] and ohmic coupling effects between HVDC and AC lines [21]. Ohmic coupling driven by corona effects can be caused by high voltage direct current (HVDC) systems which are in close proximity to conventional AC systems. This constellation can occur if an AC system on an existing tower is replaced by an HVDC system [22]. A field test on a short transmission line shows a weather dependent, corona driven DC coupling from an HVDC line to a (in this setup) grounded AC line. The DC-coupling can rise to several mA / km [21], because both, transmission lines and transformer windings represent a low ohmic path to ground.

### 4.1 EXPERIMENTAL SETUP

The evaluation of DC influences on power transformers is performed by using two identical 3-limb 30 MVA, Yy0 110/10 kV transformers. The transformers are connected in back-to-back, meaning they are connected on the 110 kV level, see Figure 13. The transformer T1 in the series

connection is powered by a three-phase voltage source on its 10 kV level. T1 provides the magnetisation current of transformer T2 which is used in open loop. The on-load tap changer position of both transformers is constant during the measurement (middle position). The star point of transformer T1 is grounded permanently. A current source inserts DC through the star point connection. Resistors $R_{sh}$ are used in the interconnections between the 110 kV bushings to force the desired DC distribution in the 110 kV phases. They consist of a variable resistor and a constant 0.1 Ω shunt which is used for current measurement. The current measurement system is isolated to ground by an optical fibre; the phase voltages are measured using capacitive dividers.

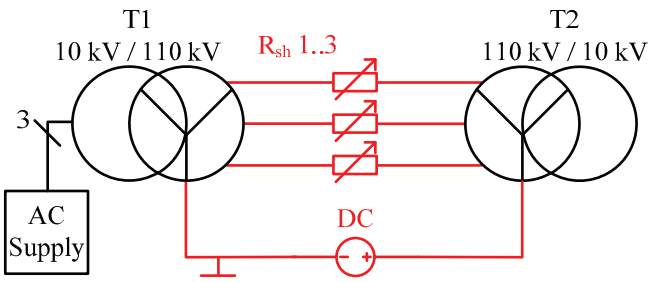


**Figure 13.** DC test setup consisting of two 3-limb 110 kV / 10 kV transformers connected on 110 kV (back-to-back). T1 with AC supply, T2 without attached load. DC injection through the star points. DC distribution by variable shunt resistors $R_{sh,1..3}$.

### 4.2 DC SCENARIOS

Two different types of scenarios are considered:

- Symmetrical scenarios; DC (and hence all magnetic direct fluxes) are approx. equally distributed.
- Asymmetrical scenarios; DC on each phase depends on the additional shunt resistors.

Table 1 shows the overall DC of the star point $I_{DC,total}$ for symmetrical scenarios, the resulting phase current $I_{DC,phase}$ and for reference the ratio between $I_{DC,phase}$ and the total magnetisation current ($I_{mag,total}$ = 700 mA @ 110 kV) for each phase. Table 2 shows the overall DC of the star point $I_{DC,total}$ for asymmetrical scenarios and the resulting current $I_{DC,phase1,2,3}$ for each phase. The relative DC distribution of scenario 1 and 2 is the same; both with higher currents on outer phase 3. Scenario 3 evaluates a setup injecting a high current into the middle phase. In scenarios 4 and 5 the middle and one outer phase share the same DC.

### 4.3 INFLUENCES ON MECHANICAL OSCILLATIONS

Accelerometers measure mechanical tank oscillations on both transformer tanks. The electric frequency of the AC supply is $f_{n,electric}$ = 50 Hz; the basic mechanical frequency $f_{mech}$ = 100 Hz.

Two types of frequencies are considered. The already discussed even harmonics (100 Hz, 200 Hz, etc.) and additional frequencies, which occur due to DC superimposition. These are the basic subharmonic $f_{sub,mech}$ = 50 Hz and odd harmonics (150 Hz, 250 Hz, etc.). The subharmonics occur due to the offset caused by DC. Therefore, the magnetic field strength $H$ is higher in one half-period than in the other which leads to an asymmetrical magnetic flux density. If the applied DC is sufficient, half-wave saturation effects can occur. Half-wave saturation of phase 3 is shown in Figure 14 for scenario 2. The equivalent hysteresis loop is derived from the measured HV current (AC+DC) on the x-axis and the integrated signal of the measured phase-to-ground voltage on the y-axis during one period. The horizontal shift to the left is caused by $|I_{DC,phase3}|$ = 480 mA.

**Table 1.** Symmetrical DC injection equally distributed on all phases.

| $I_{DC,total}$ / mA | $I_{DC,phase}$ / mA | Relative to $I_{mag,110\ kV}$ |
|---|---|---|
| 630 | 210 | 90 % |
| 2400 | 800 | 343 % |

**Table 2.** Asymmetrical DC injection scenarios. Entire DC and DC per phase

| Scenario No. | $I_{DC,total}$ / mA | $I_{DC,phase1}$ / mA | $I_{DC,phase2}$ / mA | $I_{DC,phase3}$ / mA |
|---|---|---|---|---|
| 1 | 219 | 22 | 22 | 175 |
| 2 | 600 | 60 | 60 | 480 |
| 3 | 369 | 37 | 295 | 37 |
| 4 | 370 | 22 | 174 | 174 |
| 5 | 600 | 36 | 282 | 282 |

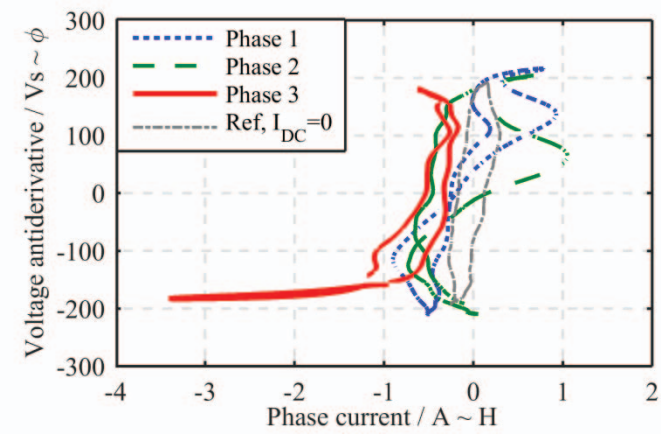


**Figure 14.** Equivalent hysteresis loop on 10 kV side at asymmetrical DC injection, scenario 2 from Table 2 and Reference without DC from phase 3.

The uneven magnetic flux density causes an asymmetrical strain in the core sheets, see Figure 1. This leads to additional mechanical frequencies equal to the electric excitation (50 Hz) and odd harmonics (150 Hz, etc.) [15]. Figure 15 illustrates the changes with and without superimposed asymmetrical DC.

The frequency behaviour of both transformers is similar. Therefore, only the signal power of transformer T1 is

considered. Figure 16 shows the relative signal power distribution of mechanical oscillation spectrum at symmetrical DC scenarios which can occur e.g. at GIC events. No significant changes in the mechanical oscillations spectrum arise. Even harmonics cover above 95 % of the acceleration signal. Odd harmonics vary between 2 – 4 % which covers measuring uncertainty. Odd harmonics do not occur because there is no significant direct flux component in the core: DC in each phase causes a magnetic flux in the same direction. The ampere sources block each other's flux and the magnetic direct flux is forced to leave core material to close its loop. No interference with the core material occurs, if the superimposed direct flux is mainly stray flux in core and limbs.

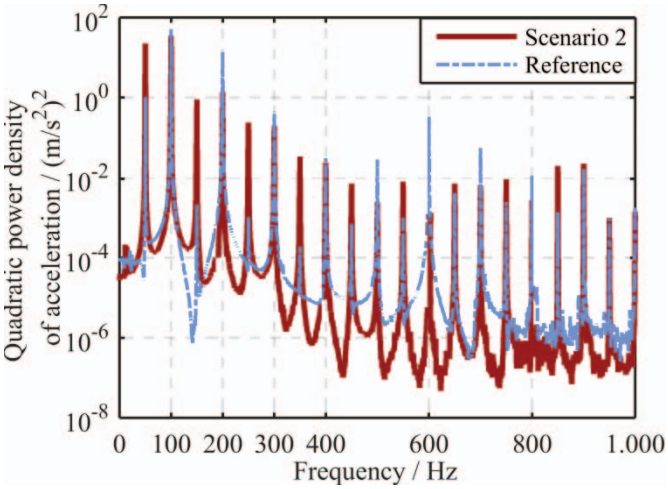


**Figure 15.** Frequency spectrum of the quadratic power density (acceleration) of reference ($U$=$U_N$, $I_{DC}$=0) and asymmetrical DC of scenario 2 from Table 2.

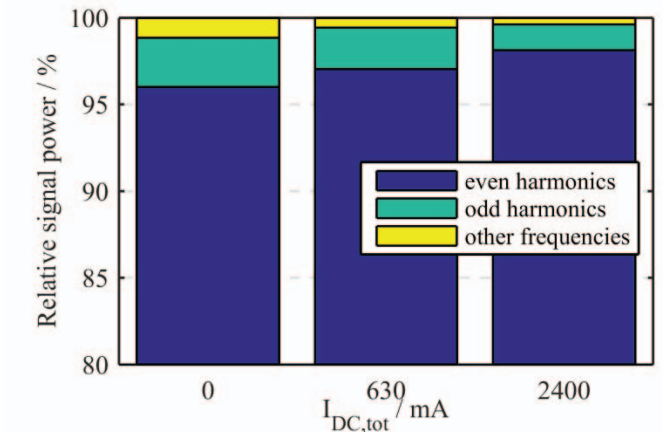


**Figure 16.** Relative signal power distribution of acceleration's even and odd harmonic content at symmetrical injection of DC, see Table 1.

Mechanical oscillations change significantly at asymmetrical DC scenarios typical for HVDC line coupling [21]. The new operating point (see Figure 1) leads to high signal powers of 50 Hz and odd harmonics. Odd components cover between 10 % (scenario 1) and approx. 40 % (scenario 2) of the acceleration signal, see Figure 17. The fraction of odd harmonics mainly depends on the asymmetrical DC distribution on the phases. Higher asymmetries lead to rising odd harmonics, see scenario 2 (worst case) compared to scenario 5. The influence of the overall $I_{DC,total}$ also depends mainly on the DC distribution: the effect of the same overall $I_{DC,total}$ is small (comparing scenarios 4 and 5), whereas the triplication to $I_{DC,total}$ = 600 mA from scenario 1 to 2 leads to major harmonic changes.

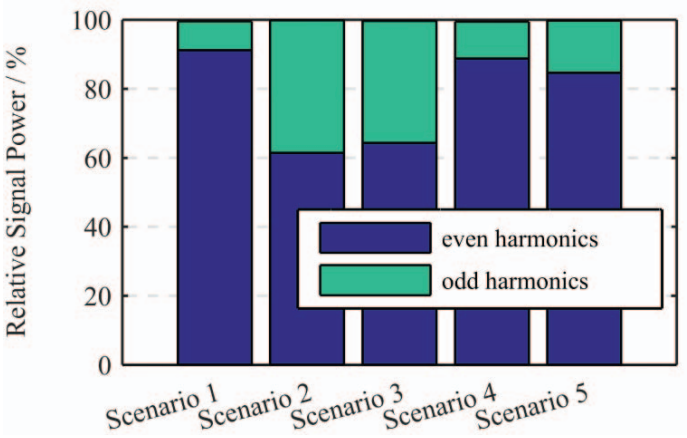


**Figure 17.** Relative signal power distribution of acceleration's even and odd harmonic content at different asymmetrical DC scenarios, see Table 2. Other frequencies not shown ( < 1%)

## 5 CONCLUSION

Mechanical changes in the active part influence mechanical oscillations on both the core itself and on the transformer's tank wall. The considered setup determines changes of the core's clamping forces. Mechanical changes can be detected using tank wall mounted acceleration sensors. The coupling from core to tank wall is influenced by the entire coupling path which denies a quantitative correlation between core and tank oscillations. Therefore, local tank wall acceleration measurement strongly depends on sensor positions.

A comparison of 10 different positions on a power transformer tank wall provides no evident correlation between single positions. Additional parameters influence the acceleration measurements, too. Currents lead to additional winding oscillations which imply a dependency to the transformer's load. Due to the material dependent thermal expansion coefficients load dependent losses and cooling systems also influence the signal coupling and hence measurement results. Mechanical oscillations are not strongly influenced by the position of the on-load tap changer (OLTC), if the OLTC regulator is set to compensate reactive power which leads to an approx. constant magnetic flux density in the core. It is advisable to use the basic mechanical frequency which is the doubled electrical frequency. Harmonics can occur due to several effects, for example the non-linearity of magnetostriction and modal frequencies of the transformer tank. Hence, an explicit correlation to the active part is not provided. Concluding, mechanical oscillation measurement seems suited for monitoring if oscillations of a single asset are evaluated over time (trend analysis) in a similar fashion like in frequency response analysis (FRA): the time dependent asset behaviour can be compared to a reference (in FRA called footprint) [23].

Undesirable DC in transformer windings can occur due to geomagnetically induced currents or by line coupling from nearby HVDC systems. If the DC on all phases is of similar magnitude and orientation, the resulting direct magnetic flux is forced into the stray field and no significant interactions occur at transformers with 3-limb geometry. Asymmetrical DC distributions lead to significant changes. Nominal mechanical oscillations are superimposed with subharmonic contents which can cover up to 40 % of the entire measured signal power. The effect depends mainly on the individual distribution of DC on the phases. These effects occur even if the DC components smaller than the transformer's magnetisation current. The discussed DC driven observations only apply to 3-limb transformers. Other core geometries, for example 5-limb transformers, which are regularly used in Europe, will provide a different behaviour due to their additional outer unwound limbs.

## REFERENCES


[1] International Electrotechnical Commision, IEC 60076-10 Power Transformers Part10: Determination of sound levels, 2001.

[2] R. Henshell, P. Bennett, H. McCallion and M. Milner, "Natural Frequencies and Mode Shapes of Vibration of Transformer Cores", Proc.IEE (UK), pp. 2133-2139, 1965.

[3] M. Wang, A.J. Vandermaar and K.D. Srivastava, "Review of Condition Assessment of Power Transformers in Service", IEEE Electr. Insul. Mag., Vol.18, No. 6, pp. 12- 25, 2002.

[4] E. Gockenbach and H. Borsi, "Condition monitoring and diagnosis of power transformers", Int'l. Sympos. Electrical Insulating Materials, pp. 16-19, 2008.

[5] IEEE Power and Energy Soc., IEEE Guide for the Interpretation of Gases Generated in Oil-Immersed Transformers, C57.104, New York, USA, 2009.

[6] International Electrotechnical Commission, IEC 60270 High-Voltage Test Techniques-Partial Discharge Measurements, 3. Edition, Geneva, Switzerland, 2000.

[7] CIGRÉ, Brochure 342-Mechanical Condition Assessment of Transformer Windings using Frequency Response Analysis (FRA), SC A2 WG A2.26, 2008.

[8] J. Shengchang, S. Ping, L. Yanming, X. Dake and C. Junling, "The vibration measuring system for monitoring core and winding condition of power transformer", Int'l. Sympos. Electr. Insulating Materials, pp. 849 - 852, 2001.

[9] B. García, J. Burgo, and Á. Alonso, "Transformer Tank Vibration Modeling as a Method of Detecting Winding Deformations Part I: Theoretical Foundation", IEEE Trans. Power Delivery, Vol. 21, No. 1, pp. 157-163, 2006.

[10] B. García, J. Burgo, and Á. Alonso, "Transformer Tank Vibration Modeling as a Method of Detecting Winding Deformations-Part II: Experimental Verification", IEEE Trans. Power Delivery, Vol. 21, No. 1, pp. 164 - 169, 2006.

[11] H.L. Rivera, J.A. Garcia-Souto and J. Sanz, "Measurements of mechanical vibrations at magnetic cores of power transformers with fiber-optic interferometric intrinsic sensor", IEEE J. Selected Topics in Quantum Electronics, Vol. 6, No. 5, pp. 788-797, 2000.

[12] P. Kung, L. Wang and M.I. Comanici, "Fiber optics temperature/vibration and moisture monitoring in power transformers", IEEE Electrical Insulation. Conference, pp. 280-284, 2011.

[13] S. Borucki, "Diagnosis of Technical Condition of Power Transformers Based on the Analysis of Vibroacoustic Signals Measued in Transient Operating Conditions", IEEE Trans. Power Delivery, Vol. 27, No. 2, pp. 670-676, 2012.

[14] G. Fasching, *Materials for Electrical Engineering*, Vienna: Springer Wien, New York, 2005.

[15] International Electrotechnical Commision, IEC 60076-10-1 Determination of Sound Levels Application Guide, 2005-10.

[16] M. Beltle and S. Tenbohlen, "Usability of Vibration Measurement for Power Transformer Diagnosis and Monitoring", Int'l. Conf. Condition Monitoring and Diagnosis, Bali, Indonesia, pp. 281-284, 2012.

[17] A. Hackl and P. Hamberger, "Investigation of surface velocity pattern of power transformers tanks", XIX Int'l. Conf. Electr. Machines (ICEM), Rome, pp. 1-3, 2010.

[18] R.S. Girgis, M.S. Bernesjö, S. Thomas, J. Anger, D. Chu and H.R. Moore, "Development of Ultra-Low-Noise Transformer Technology", IEEE Trans. Power Delivery, Vol. 26, No. 1, pp. 228-234, 2011.

[19] R. Girgis and K. Vedante, "Effects of GIC on power transformers and power systems", IEEE PES Transmission and Distribution Conference and Exposition, Orlando FL, pp. 1-8, 2012.

[20] Geomagnetic Disturbances: Their Impact on the Power Grid", IEEE Power and Energy Magazine, Vol. 11 No. 4, pp. 71-78, 2013.

[21] B. Rusek, C. Neumman, S. Steevems, U. Sundermann, K. Kleinekorte, J. Wulff, F. Jenau, K.-H.Weck, UOhmic coupling between AC and DC circuits on hybrid overhead lines", Cigré 2013, Auckland, NZ, 2013.

[22] B. Sander, J. Lundquist, I. Gutman, C. Neumann, B. Rusek and K.-H. Weck, "Conversion of AC multi-circuit lines to AC-DC hybrid lines with respect to the environmental impact", Cigré Study committee B2, B2-105, 2014.

[23] T. Leibfried and K. Feser, "Monitoring of Power Transformers using the Transfer Function Method", IEEE Trans. Power Delivery Vol. 14, No. 4, pp. 1333-1341, 1999.


**Michael Beltle** received the Dipl.-Ing. degree in electrical engineering from the University of Stuttgart, Germany, in 2009. In his diploma thesis he was involved in determining degrading effects of electrostatic discharges on microcontrollers in automotive applications. He has been an Academic Researcher with the Institute of Power Transmission and High Voltage Technology, University of Stuttgart where he is involved in the field of power transformer diagnostics and determines the long-term development of partial discharges and investigates the mechanical vibrations of active parts of transformers. He is a member of CIGRE and the German Power Engineering Society VDE-ETG.

**Stefan Tenbohlen** (M'04-SM'14) received his Diploma and Dr.-Ing. degrees from the Technical University of Aachen, Germany, in 1992 and 1997, respectively. In 1997 he joined ALSTOM Schorch Transformatoren GmbH, Mönchengladbach, Germany, where he was responsible for basic research and product development. From 2002 to 2004 he was the head of the electrical and mechanical design department. In 2004 he was appointed to a professorship and head of the institute of Power Transmission and High Voltage Technology of the University of Stuttgart, Germany. In this position his main research fields are high voltage technique, power transmission and electromagnetic compatibility (EMC). Prof. Tenbohlen holds several patents and published more than 300 papers. He is member of CIGRE SC A2 (Power Transformers), German committees of A2, D1 (Emerging Technologies), C4 (System Technical Performance), several international working groups and the chairman of German Power Engineering Society VDE-ETG FB Q2 (Materials, Electrical Insulations and Diagnostics).